PROCEEDINGS OF SCIENCE

Neutron Propagation Time Distribution Measured by Various Neutron Monitor Counters Relative to Direction-Tracked Charged Atmospheric Secondaries

Koth Amratisha,[a,*] **Kullapha Chaiwongkhot,**[a] **Jidapa Lakronwat,**[a,b] **Kunlanan Puprasit,**[a,c] **Achariyaporn Janmaneeporn**[d] **and David Ruffolo**[a]

[a] *Department of Physics, Faculty of Science, Mahidol University, Bangkok 10400, Thailand*
[b] *Department of Physics, Faculty of Science, Kasetsart University, Bangkok 10900, Thailand*
[c] *National Astronomical Research Institute of Thailand (NARIT), Chiang Mai 50180, Thailand*
[d] *400/4, Pibulsongkram Road, Nakhon Ratchasima, 30000, Thailand*

E-mail: koth.ama@student.mahidol.edu, david.ruf@mahidol.ac.th

A ground-based neutron monitor detects atmospheric secondary particles from cosmic ray showers that interact in the monitor to produce neutrons, which can propagate to and be detected by neighboring neutron monitor counters. To study the propagation time distribution, the arrival time and position of atmospheric secondaries are needed. In this work, we used a plastic scintillator bar with two silicon photomultipliers attached at opposite ends to track the position of charged secondary particle passage. Triggering together with a small scintillator above that scintillator bar, we determined the trajectories of charged secondary particles and traced them to the lead producer of the Princess Sirindhorn Neutron Monitor (PSNM). With such timing and position data, we can study the propagation time distribution measured by various neutron monitor counters and compare that with the two-dimensional diffusion-absorption model proposed in previous work.

38th International Cosmic Ray Conference (ICRC2023)
26 July - 3 August, 2023
Nagoya, Japan

*Speaker

PoS(ICRC2023)110

1. Introduction

Cosmic rays are high-energy particles originating from energetic sources. They can be directly detected on board satellites in space, which allows accurate determination of cosmic ray species. However, cosmic ray flux decreases with energy, especially above 1 GeV[1], so small detectors on board satellites are not adequate for precise monitoring of time variations in the fluxes of those high-energy cosmic rays. Ground-based detectors do not have such size limitations. Moreover, cosmic rays with energy in the GeV range or higher interact with air molecules when arriving at Earth and generate showers of secondary cosmic rays. These cosmic ray showers can cover an area in the range of a few square kilometers, increasing the effective area of the detector [2]. A major component of the cosmic ray shower are neutrons, which can be detected by neutron monitors with hourly count rate over 10^6 making neutron monitors the main instrument for monitoring the temporal variation of GeV-range cosmic rays [3]. Although ground-based neutron monitors cannot directly measure the energy of the primary cosmic rays, Earth's magnetic field prevents cosmic rays below the local cutoff rigidity (where the rigidity $P = pc/q$ for the cosmic ray momentum p and charge q) from entering the atmosphere. Therefore, neutron monitor stations are operating worldwide to monitor cosmic rays at different local cutoff rigidity values[4].

Typically neutron monitors contain a lead producer which interacts with incoming secondary particles to generate MeV-range neutrons that are then detected by proportional counter tubes. The generated neutrons are scattered and propagate throughout the neutron monitor. The escape of produced neutrons is reduced by an outer layer of polyethylene reflector. The neutron time delay is the time between successive neutron counts, which is the result of the neutron propagation time and can be used to study galactic cosmic ray (GCR) spectral variation [5, 6]. Since secondary particles often travel near the speed of light, we interpreted neutron timing relative to a secondary particle trigger as the propagation time of produced neutrons [7, 8]. The non-destructive detection of charged secondary particles above the neutron monitor can provide timing information for the study of produced neutron propagation. When a charged particle such as a proton travels within scintillator material, it deposits some of its energy and generates photons, allowing its detection. While most neutron monitor counts result from atmospheric secondary neutrons, 15% of the PSNM count rate is contributed by secondary protons and about 1.8% by secondary muons [9]. The propagation of neutrons generated by interactions of secondary protons in the lead producer should be similar to that for neutrons generated by interactions of secondary neutrons, which account for most neutron monitor counts.

In our previous work [10], we studied the propagation time distribution of neutrons associated with charged particles entering a neutron monitor. A small scintillator was placed on top of PSNM for non-destructive detection of charged secondary particles, which provided a timing trigger for neutron propagation time measurement. That work also presented an analytic model of the neutron propagation and Monte Carlo simulation results. In this work, we aim to improve upon that work and develop a position sensitive scintillator that can determine the trajectory of secondary charged particles. By comparing signals from two readouts from the opposite ends of a scintillator bar, we can estimate the positions where charged particles crossed the scintillator and entered the neutron monitor. We measured neutron pulses from various PSNM counters in order to study the propagation time as a function of distance from the inferred impact location of the charged

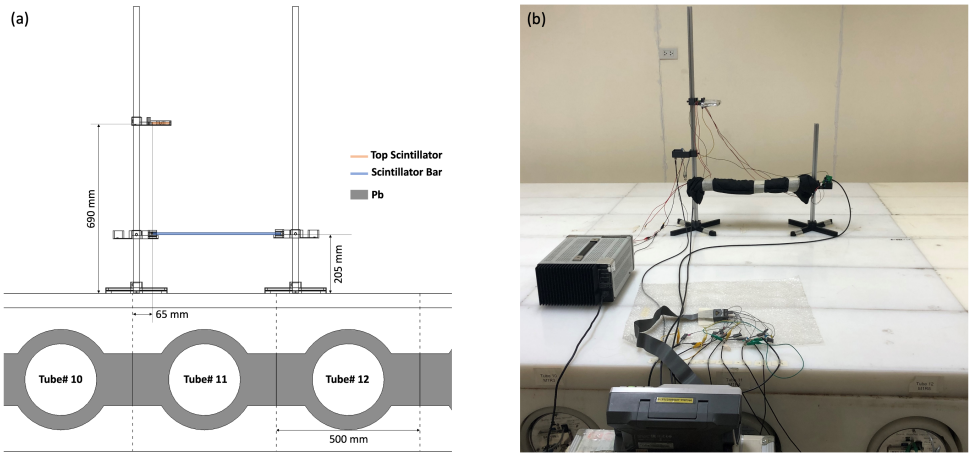

Figure 1: (a) Drawing of the placement of the top scintillator (highlighted in orange) and the scintillator bar (highlighted in blue) above a neutron monitor used in the experiment. (b) Photograph of scintillators set up on top of PSNM.

secondary particle. This way, we will be able to compare neutron time distribution with the position or angle of secondary particle incidence.

2. Methods

2.1 Experimental setup

PSNM is a NM64-type neutron monitor [7] containing 18 BP-28 neutron-sensitive proportional counters (Chalk River Laboratories, Canada) filled with borontrifluoride (BF_3) gas at low pressure (200 mmHg) in which the boron is 95% enriched in ^{10}B. A secondary particle can disrupt a nucleus in the lead producer around a proportional counter tube and produce several MeV-range neutrons. Polyethylene reflector reflects produced neutrons and keeps them within the neutron monitor. A polyethylene moderator is inserted between the lead producer and proportional counter to reduce the neutron energy since the proportional counters are more sensitive to thermal neutrons. Neutrons can be detected in a proportional counter from the reaction

$$n + {}^{10}\mathrm{B} \longrightarrow {}^{7}\mathrm{Li} + {}^{4}\mathrm{He}$$

and ionization of the gas by the product nuclei.

The scintillator setup consists of two scintillators. A scintillator bar ($450 \times 70 \times 7$ mm^3 EJ-200 plastic scintillator bar from Eljen Technology, USA) is covered in aluminum foil with two small openings for two SiPMs (MicroFJ-60035, Onsemi, USA) attached with optical grease. A small scintillator ($60 \times 80 \times 5$ mm^3 plastic scintillator from Epic Crystal, China) was placed above the scintillator bar. The top scintillator was covered in aluminum foil and attached optically to a SiPM (MicroFJ-30035, Onsemi, USA). The placement of both scintillators on top of PSNM Tube 11 is shown in Figure 1(a). Measuring and comparing signals from SiPMs at the opposite ends can

determine the point where a charged particle passed through the scintillator bar. We set up the coincidence between the SiPM of the top scintillator and the right side SiPM of the scintillator bar corresponding to the drawing and photo in Figure 1 to provide a logic signal if the signals from both SiPMs occurred within around 1 μs. The coincident signal was used to trigger the data collection on the oscilloscope (DS1104Z Plus, Rigol, China). By using 30,000 sampling points, the shape of the signal pulses was collected within a 6-ms time window for each channel of the oscilloscope. Tracing charged particles from the top scintillator to the estimated position on the scintillator bar gives the trajectory of those particles. The analog signals from the left and right sides of the scintillator bar, and from Tube 11, were recorded together with digital signals from proportional counter Tubes 7, 9, 11, 12, 13, 14 and 18 from -1 to 5 ms relative to the trigger time, to record neutron time distributions from those counters. Digital signals from Tube 14 were anomalous and are not used in further analysis.

2.2 Position sensing calibration

A small calibration scintillator (the same model as the top scintillator) was placed under the scintillator bar, centered at 30, 128, 225, 322, and 420 mm from the left edge of the bar and signals were recorded for 4-fold coincidence between the SiPMs at the top scintillator, both ends of the scintillator bar, and the calibration scintillator. The signals were reprocessed to extract the pulse heights, peak times, and time over the threshold from SiPM pulses at the trigger time. Since the extracted data have 6 variables (3 from each of the left and right SiPMs), we used machine learning to make a model for position prediction. For each calibration position, we recorded 70 data sets. We used the scikit-learn Python library to generate a position prediction model. To find the best prediction model, we used a grid search with 5-fold cross-validation and selected the model with the highest prediction score.

3. Preliminary results

3.1 Neutron time distribution

Neutron counts from proportional counter Tubes 7, 9, 11, 12, 13, and 18 were collected from 77,849 scintillator events from June 6 to June 29, 2023. Figure 2 shows the time distribution of digital signals from PSNM proportional counters. We observed some background counts at all times from unrelated secondary particles from other cosmic ray showers. The spike from $t = 0$ to 20 μs includes prompt pulses from charged particle ionization in the proportional counters, which was also observed in previous measurements and Monte Carlo simulations [10]. For simplicity we still refer to all signals as "neutron signals". However, because of the contributions of charged-particle ionization and prompt neutrons during $t = 0$ to 20 μs, we exclude this time period from comparisons with the propagation model for slow neutrons.

In the diffusion-absorption model of Chaiwongkhot (2021)[10], the distribution of the propagation time t of slow neutrons inside the neutron monitor is related to the distance r between neutron production and detection:

$$n \propto \frac{1}{t} \exp\left(-\frac{T_r}{t}\right) \exp(-\alpha t),$$

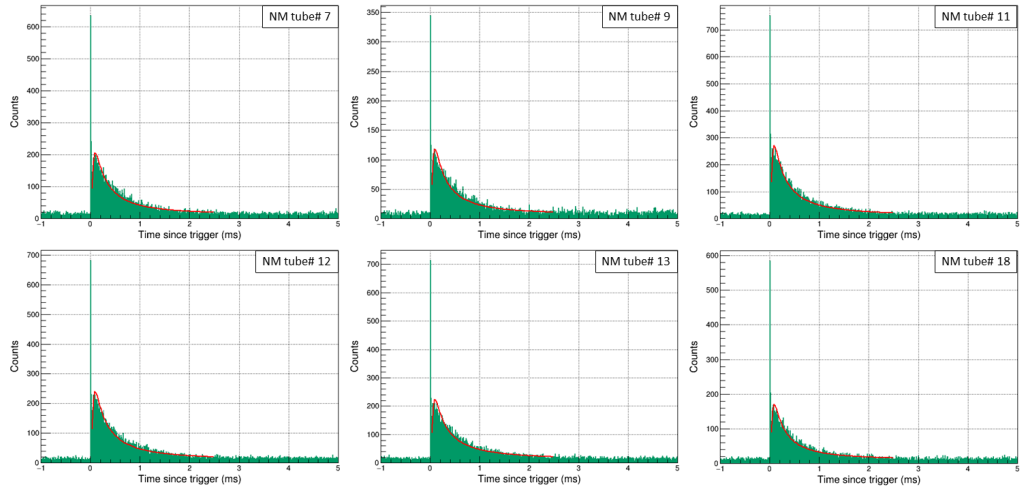

Figure 2: Time distribution of digital neutron signals from PSNM Tubes 7, 9, 11, 12, 13, and 18 relative to the charged particle trigger time. The red line indicates the fit to non-prompt signals using an analytic formula for neutron diffusion and absorption.

Tube number	T_r (ms)	α (ms)
7	0.09686	0.5706
9	0.09400	0.6206
11	0.09063	0.5154
12	0.09434	0.5053
13	0.09428	0.4546
18	0.08941	0.6427

Table 1: Neutron time distribution parameters of each proportional counters

where α is the rate of neutron absorption by materials inside the neutron monitor, including capture by ^{10}B as detected by a proportional counter. The rise time depends on the distance r as $T_r \equiv (x^2 + y^2)/(4D)$, where (x, y) is the 2D displacement in the plane perpendicular to the proportional counter wire, and D is a neutron diffusion coefficient. We use this relationship to fit the neutron time distribution for each tube to find the rise time (T_r) and the rate of absorption (α). We use the mean count rate from time -980 to -20 µs as the background level, which is subtracted before fitting. Since the secondary particles flux depends on the zenith angle, most of the events collected are for secondary particles traveling at low zenith angle[11, 12] and hitting the lead around PSNM Tube 11.

The position of neutron production is most commonly near tube 11, causing the rise time to be the lowest among nearby tubes. The neighboring tubes have significantly higher rise times. Relative to tube 11, tubes 9, 12, and 13 have almost a 4 µs increase in rise time, while tube 7 has about a 6 µs increase in rise time. However, tube 18 has slightly lower rise times than tube 11. We suspect that the reason why T_r does not continue to increase for more distant proportional counter tubes is

related to multiple secondaries from the same cosmic ray shower [13, 14], which entered the NM at different locations at times similar to the scintillator trigger time. For tubes distant from Tube 11, multiple secondary particles provide the dominant contribution to neutron signals coincident with the scintillator trigger. Those neutrons were typically produced at locations near that tube with small $x^2 + y^2$, resulting in a rise time that is not very different from that of Tube 11. In further work, we will aim to veto events with multiple secondaries, so as to study neutrons produced at the point of impact of the single charged secondary particle tracked by our scintillators, for better determination of $x^2 + y^2$ for various proportional counter tubes.

3.2 Position sensing

To study the effect of the position and angle of secondary particle events, we need to non-destructively detect them before they hit the neutron monitor. We thought a secondary particle crossing a scintillator bar should give differents readout to both ends. Signals from left and right SiPMs on the scintillator bar were collected using a calibration scintillator at one of five positions to select secondary events passing through known positions along the scintillator bar. The data set including the know calibrating scintillator position paired with 6 parameters from left and right SiPMs was fit using the random forest classifier model because this model gave the highest prediction score. The model takes the data and tries to generate the best model to determine the position (among five choices) in which the secondary particle cross the scintillator bar using pulse parameters from SiPM signals. After fitting we test the model using a test data set that was separated before the training. From our test, the average prediction score of the random forest classifier on test data sets is 0.59. The prediction of test data sets is shown in Figure 3(a). Figure 3(b) shows the prediction results for 47,412 data sets with undetermined positions along the scintillator bar. The muon flux decreases as a function of $\cos\theta$, where θ is the zenith angle [11], as does the proton flux[12]. From this relationship, we should observe a gradual decrease in the number of counts as the zenith angle increases, i.e., for a position farther from the left edge of the scintillator bar, if the prediction model is accurate. However, the prediction results did not agree. Although we observe a decrease in count rate as the zenith angle increases the prediction model favors the positions at 128 mm and 322 mm which indicate false prediction, and thus we do not trust this prediction model. More investigation is required for the position sensing model.

3.3 Future plans

The main objectives of this work are to develop position sensitive charged particle detectors and to measure the neutron propagation time to different locations in a neutron monitor, which can be compared with an analytical model and Monte Carlo simulation results. We plan to investigate more ways to determine the trajectories of charged particles passing scintillators to tell us the position and angle at which the secondary particle hits the lead producer, so we can compare neutron time distributions for different positions. Furthermore, using detailed information collected by PSNM for events with many coincident neutron counts [14], we can veto events that clearly involve multiple secondaries to better focus on neutrons produced by single charged secondaries of known position and angle. In this way, we aim to determine the relationship between the neutron time distribution and the angle and position of secondary particle incidence.

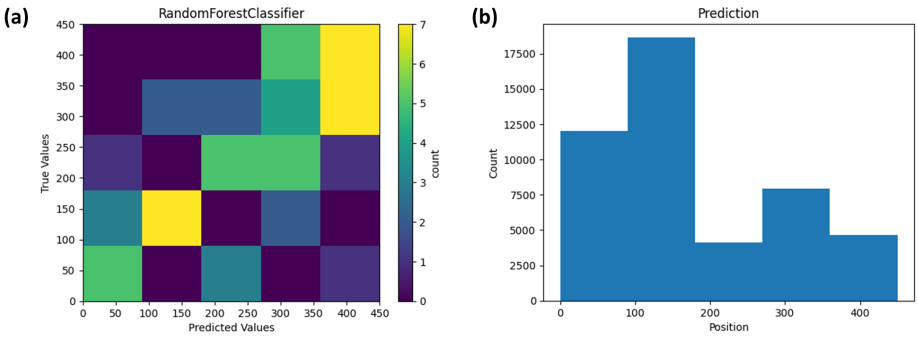

Figure 3: (a) A 2D histogram showing the results of prediction of test data for the position along the scintillator. (b) The distribution of predicted positions from real data.

Acknowledgments

Partially supported by the National Science and Technology Development Agency (NSTDA) and the National Research Council of Thailand (NRCT) under the High-Potential Research Team Grant Program (N42A650868), and from the NSRF via the Program Management Unit for Human Resources & Institutional Development, Research and Innovation (B37G660015). Support was also provided to J.L. from the Development and Promotion of Science and Technology Talents Project (DPST) and to K.P. from postdoctoral research sponsorship of Mahidol University. Special thanks to the National Research Council of Thailand for their financial support that facilitated the success of our research through the Hub of Talents in Spacecraft Scientific Payload, Grant No. N35E660131, and the Hub of Knowledge in Space Technology and its Application, Grant No. N35E660132.

References

[1] W. Bietenholz, *The most powerful particles in the universe: A cosmic smash*, *Revista Cubana de Fisica* **31** (2013) .

[2] J.A. Simpson, *The latitude dependence of neutron densities in the atmosphere as a function of altitude*, *Phys. Rev.* **73** (1948) 1389.

[3] J.A. Simpson, *The cosmic ray nucleonic component: The invention and scientific uses of the neutron monitor – (keynote lecture)*, *Space Science Reviews* **93** (2000) .

[4] D. Ruffolo, *Time variations in galactic cosmic rays as measured from southeast asia*, *Journal of Physics: Conference Series* **1572** (2020) 012087.

[5] D. Ruffolo, A. Sáiz, P.-S. Mangeard, N. Kamyan, P. Muangha, T. Nutaro et al., *Monitoring short-term cosmic-ray spectral variations using neutron monitor time-delay measurements*, *The Astrophysical Journal* **817** (2016) 38.

[6] C. Banglieng, H. Janthaloet, D. Ruffolo, A. Sáiz, W. Mitthumsiri, P. Muangha et al., *Tracking cosmic-ray spectral variation during 2007–2018 using neutron monitor time-delay measurements*, *The Astrophysical Journal* **890** (2020) 21.

[7] C.J. Hatton and H. Carmichael, *Experimental investigation of the nm-64 neutron monitor*, *Canadian Journal of Physics* **42** (1964) 2443 [https://doi.org/10.1139/p64-222].

[8] V.P. Antonova, A.P. Chubenko, S.V. Kryukov, N.M. Nesterova, A.L. Shepetov, V.V. Piscal et al., *Anomalous time structure of extensive air shower particle flows in the knee region of primary cosmic ray spectrum*, *Journal of Physics G: Nuclear and Particle Physics* **28** (2002) 251.

[9] N. Aiemsa-ad, D. Ruffolo, A. Sáiz, P.-S. Mangeard, T. Nutaro, W. Nuntiyakul et al., *Measurement and simulation of neutron monitor count rate dependence on surrounding structure*, *Journal of Geophysical Research: Space Physics* **120** (2015) 5253 [https://agupubs.onlinelibrary.wiley.com/doi/pdf/10.1002/2015JA021249].

[10] K. Chaiwongkhot, D. Ruffolo, W. Yamwong, J. Prabket, P.-S. Mangeard, A. Sáiz et al., *Measurement and simulation of the neutron propagation time distribution inside a neutron monitor*, *Astroparticle Physics* **132** (2021) 102617.

[11] M. Bahmanabadi, *A method for determining the angular distribution of atmospheric muons using a cosmic ray telescope*, *Nuclear Instruments and Methods in Physics Research Section A: Accelerators, Spectrometers, Detectors and Associated Equipment* **916** (2019) 1.

[12] T. Sanuki, M. Fujikawa, H. Matsunaga, K. Abe, K. Anraku, H. Fuke et al., *Measurement of cosmic-ray proton and antiproton spectra at mountain altitude*, *Physics Letters B* **577** (2003) 10.

[13] K. Chaiwongkhot, D. Ruffolo, A. Sáiz, W. Mitthumsiri, P. Chaiwongkhot, C. Banglieng et al., *these proceedings*, .

[14] P. Evenson, J. Clem, P.-S. Mangeard, W. Nuntiyakul, D. Ruffolo, A. Sáiz et al., *these proceedings*, .

PoS(ICRC2023)110